Dipole anisotropy in flux density and source count distribution in radio NVSS data

Rahul Kothari, Abhishek Naskar, Prabhakar Tiwari, Sharvari Nadkarni-Ghosh and Pankaj Jain

Department of Physics, Indian Institute of Technology, Kanpur - 208016, India

26 June,2013

ABSTRACT

We study the dipole anisotropy in the number counts and flux density in the NRAO VLA Sky Survey (NVSS) data. The dipole anisotropy is expected due to our local motion with respect to the CMBR rest frame. In agreement with earlier results, we find that the amplitude of anisotropy is significantly larger in comparison to the prediction based on CMBR measurements. The direction, however, is found to be in good agreement. The local speed extracted using flux density is found to be somewhat smaller in comparison to earlier results, but still much larger in comparison to the CMBR expectation. We attribute this partially to the revised formula we use to relate the dipole amplitude to speed in this case. The significance of detection of anisotropy is found to be 3 σ for flux density and $3.5 - 5.4$ σ for source counts, depending on the cut on flux density. Furthermore the extracted speed using flux density differs by 2.5 σ from the speed corresponding to CMBR. The corresponding significance for number counts is $4 - 5$ σ. We find that the results are relatively insensitive to the lower limit imposed on the flux density. Our results suggest that the Universe is intrinsically anisotropic with the axis of anisotropy axis pointing roughly towards the Virgo cluster.

Subject headings: radio galaxies: high-redshift, galaxies: active

1. Introduction

The observed dipole anisotropy in the Cosmic Microwave Background Radiation (CMBR) is generally interpreted in terms of the motion of the solar system with respect to the CMBR rest frame. The corresponding speed is found to be (369$\pm$1 km s^{-1}) in the direction, $RA = 168^o$, $DEC = -7^o$. We expect that, at large distance scales, galaxies would be distributed isotropically with respect to the CMBR rest frame. However, due to Doppler and aberration effect, they would also show an anisotropic distribution (Ellis & Baldwin 1984). This effect should be observable both in the number counts and intensity of sources at high redshifts. The resulting anisotropy has been probed both in radio and optical surveys. Using the NRAO VLA Sky Survey (NVSS) (Condon et al. 1998), Blake & Wall (2002) reported a positive detection of dipole anisotropy in

the radio source count at roughly 3σ confidence level with the direction in reasonable agreement with the CMBR. The speed was found to be roughly 1.5 to 2 times larger in comparison to that extracted from the CMBR dipole. In an independent analysis of the same data, using both number counts and sky brightness, Singal (2011) reported a much larger value of the local velocity ($1600\pm$ 400 km s^{-1}), which is roughly four times larger than the prediction from CMBR observations. The direction was found to be consistent with the CMBR dipole. The results using number counts and sky brightness agreed with one another within errors, with the sky brightness based analyses yielding a larger value. Finally, Gibelyou & Huterer (2012) find a result almost six times larger than that found in (Blake & Wall 2002).

The current situation with radio analysis is clearly puzzling. All the three analysis (Blake & Wall 2002; Singal 2011; Gibelyou & Huterer 2012) find the direction in agreement with CMBR. However all three disagree with one another on the extracted speed. Whereas, Blake & Wall (2002) claim results roughly consistent with CMBR, the large amplitude found in Singal (2011) suggests a potential violation of the cosmological principle. Gibelyou & Huterer (2012) attribute their deviation from CMBR predictions to observational bias. The low value of speed extracted by Blake & Wall (2002) might have a simple explanation, as observed in (Singal 2011). The amplitude of the dipole quoted in (Blake & Wall 2002) is consistent with that obtained in (Singal 2011). The difference of a factor of approximately two arises in the extracted speed. This might be traced to extra factor of two present in the relationship between the dipole amplitude and the speed quoted in (Blake & Wall 2002) in comparison to that given in (Ellis & Baldwin 1984).

In the present paper we revisit this problem in an attempt to get a consistent result. We extract the dipole from data by making a spherical harmonic decomposition, which is also the procedure used in (Blake & Wall 2002). We impose the same cuts on data as in (Blake & Wall 2002). We remove sources with flux density less than 10 mJy and those lying within 15^o of the galactic plane. Furthermore we remove sources which are likely to belong to the local supercluster. The final data set covers the sky unevenly. We treat the masked regions by filling them randomly by the data extracted from the remaining pixels. This preserves the distribution of the data in the masked regions. This procedure differs from that adopted in (Blake & Wall 2002) who analyze masked sky data directly. We have verified that if we follow the masked sky analysis used in (Blake & Wall 2002), the results remain same within errors. We find the full sky analysis convenient since it allows us to probe the dipole directly. Furthermore any bias that might be generated by random filled can be determined by simulations and subtracted from the final result.

Our procedure differs from earlier papers (Blake & Wall 2002; Singal 2011; Gibelyou & Huterer 2012) in several respects. We show that the predicted kinematic dipole anisotropy in observed flux is different from that in number counts. This point has been missed in all the earlier papers. We independently extract the dipole anisotropy from number counts and flux density. We also report the statistical significance of the extracted dipole anisotropy. This important parameter has not been reported in any of the earlier papers which only list the sigma value with which the extracted dipole differs from that predicted by CMBR. Furthermore the bias in the extracted magnitude and

direction of velocity, generated due to partial sky data, is consistently computed by simulations and subtracted from the final results. Assuming the presence of an intrinsic dipole anisotropy in data, as suggested in (Singal 2011), we present a method to independently extract the intrinsic and kinematic dipole. Finally we present a method based on mean flux density per source, which can be used even in the case of uneven distribution of source counts.

The results obtained in (Singal 2011) suggest the possibility that the Universe may be intrinsically anisotropic with the preferred axis approximately in the direction of the CMBR dipole. There already exist considerable evidence in favor of such a hypothesis (Ralston & Jain 2004). The radio polarization offset angles with respect to the galaxy axis show a dipole anisotropy with preferred axis closely aligned with CMBR dipole (Jain & Ralston 1998). The Cosmic Microwave Background Radiation (CMBR) quadrupole and octupole also indicate a preferred axis pointing in this direction (de Oliveira-Costa et al. 2004; Schwarz et al. 2004). The two point correlations in the quasar optical polarizations (Hutsemékers 1998; Hutsemékers & Lamy 2001; Jain et al. 2004) also indicate a preferred axis closely aligned with CMBR dipole axis (Ralston & Jain 2004). Furthermore the cluster peculiar velocities (Kashlinsky et al. 2009b,a) at large distances also indicate a direction close to the CMBR dipole.

2. Theory

The absolute cosmological frame of reference can be determined by observing the dipole anisotropy of CMBR or radio data. The assumption here is that there is no intrinsic dipole anisotropy and the observed dipole is purely due to local motion which causes Doppler and aberration effect. The very first attempt to determine the local motion began with Ellis & Baldwin (1984). An observer moving with a velocity $\vec{v}$ ($v << c$), sees the sky brighter in forward direction due to Doppler boosting and aberration effect. The flux density of radio sources follows a power-law dependence on frequency ν, $S \propto \nu^{-\alpha}$, with $\alpha \approx 0.75$ (Ellis & Baldwin 1984). Let $N(> S)$ represent the integrated source population above intensity (S). This can also be well represented by a power-law $N(> S) \propto S^{-x}$ with $x \sim 1$ (Ellis & Baldwin 1984). Here we determine the value of x directly by fitting a power law to the data in the neighbourhood of the lower limit on the flux density. For an observer moving with a velocity v, the Doppler shift in the frequency (ν_{rest}) is $\nu_{obs} = \nu_{rest}\delta$, where $\delta \approx [1 + (v/c)cos\theta]$, at leading order. Hence,

$$S_{obs} = S_{rest}\delta^{1+\alpha} \tag{1}$$

at a fixed frequency in observer frame. Furthermore, the aberration effect changes the solid angle in the direction of motion $d\Omega_{obs} = d\Omega_{rest}\delta^{-2}$. Hence the net effect of Doppler boosting and aberration produces a dipole anisotropy in source count, given by,

$$\vec{D}_N(v) = [2 + x(1 + \alpha)](\vec{v}/c). \tag{2}$$

In (Ellis & Baldwin 1984) it has been pointed out that to measure the dipole anisotropy at 3σ significance level one needs to have $\sim 2 \times 10^5$ number of radio sources. However such a large

catalogue was not available at that time. The authors analyzed 4C catalogue data (4844 sources), and determined the local velocity as 551 ± 448 km s^{-1}.

We next determine the anisotropy, $\vec{D}_S(v)$, in the observed flux density or sky brightness due to Doppler and aberration effect. Here the observable, S_I, is the flux density, integrated over sources per unit area. We divide the sky into a large number of equal area pixels. In each pixel, S_I is equal to the sum of flux densities of all the sources. As in the case of source count, here also we only consider sources above a limiting flux density. Given the anisotropy in source count, the Doppler effect produces an extra shift in flux density of each source, given by Eq. 1. Hence the dipole anisotropy in S_I is given by,

$$\vec{D}_S(v) = [2 + x(1+\alpha) + (1+\alpha)](\vec{v}/c). \tag{3}$$

This provides an independent method to compute the velocity of the solar system with respect to the cosmological rest frame.

Earlier analysis (Singal 2011), suggest the presence of an intrinsic dipole anisotropy in the radio data. It is very likely that the distribution of radio sources is intrinsically anisotropic. Hence let us assume the following form for the observed $D_N(obs)$.

$$\vec{D}_N(obs) = \vec{D}_0 + [2 + x(1+\alpha)](\vec{v}/c) \ , \tag{4}$$

where $\vec{D}_0$ represents the intrinsic dipole anisotropy in the flux density. Let us next assume that the intrinsic anisotropy in the sky brightness is caused entirely by the intrinsic anisotropy in the source distribution. In this case, the total dipole anisotropy in sky brightness is given by,

$$\vec{D}_S(obs) = \vec{D}_0 + [2 + x(1+\alpha) + (1+\alpha)](\vec{v}/c). \tag{5}$$

This is of course only one possible model. In general the intensities of radio sources may also be intrinsically anisotropic. Within this model, we may separate out the intrinsic dipole in number counts from the kinematic dipole. Using Eqs. 5 and 4, we can extract both $\vec{D}_0$ and velocity $\vec{v}$, directly from the radio data. The velocity $\vec{v}$ and $\vec{D}_0$ in terms of $\vec{D}_N$ and $\vec{D}_S$ are,

$$\vec{v} = \frac{[\vec{D}_S(obs) - \vec{D}_N(obs)] \times c}{1+\alpha} \tag{6}$$

and,

$$\vec{D}_0 = \frac{(2 + 2(1+\alpha))\vec{D}_N(obs) - (2 + (1+\alpha))\vec{D}_S(obs)}{1+\alpha} \tag{7}$$

The amplitude of the intrinsic dipole is denoted by D_0 and the corresponding direction parameters, (θ_I, ϕ_I).

We may also explore the anisotropy in the flux density per source, denoted by $\bar{S}$. This has the advantage that it is unaffected by anisotropic distribution of the number counts. Given a distribution of source counts, the flux density per source in any direction θ would show a dipole

anisotropy with amplitude $(1 + \alpha)v/c$, due to Doppler effect. Hence this provides an additional independent method to test the presence of kinematic dipole. In the case of the NVSS data, this procedure does not lead to a significant extraction of dipole. Hence we do not pursue it here. However it might be useful when more data becomes available.

3. The Data

The NRAO VLA Sky Survey (NVSS) (Condon et al. 1998) is a radio continuum survey covering the entire northern sky, $\delta > -40^o$. It operates at the frequency of 1.4 GHz. The NVSS catalogue contains 1773484 radio sources. Following (Blake & Wall 2002) we impose various cuts on the data. We only include sources with flux density greater than 10 mJy and less than 1000 mJy. We remove sources lying within the galactic latitude $|b| < 15°$. Furthermore, we remove the clustering dipole (Blake & Wall 2002), i.e. sources which might belong to the local supercluster. This is accomplished by removing sources within 30 arcsec of known nearby galaxies as listed in (Saunders et al. 2000) and in the third reference catalogue of bright Galaxies from (Corwin et al. 1994). Using all above cuts we have about $\sim 10^5$ sources remaining in the data set.

We use HEALPix[1] to generate the angular position on the sky with the resolution parameter Nside=32. The angular size of a pixel for Nside=32 is roughly $\sim 1.8°$. Using this resolution we fill the map with the data available. The distribution of number count in each pixel, Fig. 1, is well described by a Gaussian, as expected. We do not find any pixel with no source.

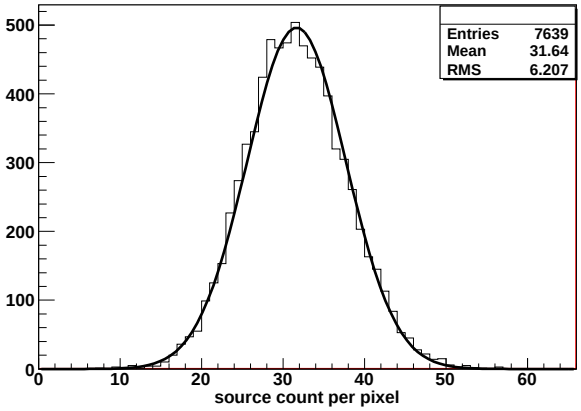

Fig. 1.— The distribution of source counts per pixel for the cut $S > 20$ mJy. The Gaussian fit to the distribution is also shown.

[1]http://healpix.jpl.nasa.gov/

4. Procedure

Let $I(\theta, \phi)$, represent the number count or flux density (S_I) as a function of the polar coordinates (θ, ϕ). We rewrite this field as $I(\theta, \phi) = I_0(1 + \Theta(\theta, \phi))$, so that the $\Theta(\theta, \phi)$ represents the fluctuations in this field. To study the correlation of this field we expand $\Theta(\theta, \phi)$ in spherical harmonics coefficients a_{lm} as,

$$\Theta(\theta, \phi) = \sum_{l=0}^{\infty} \sum_{m=-l}^{+l} a_{lm} Y_{lm}(\theta, \phi), \tag{8}$$

where $Y_{lm}(\theta, \phi)$ are the spherical harmonics. The power, C_l, in each multipole is given by,

$$C_l = \frac{1}{(2l+1)} \sum_{m=-l}^{l} |a_{lm}|^2. \tag{9}$$

A significant value of C_l indicates anisotropy at a scale $\sim (\pi/l)$ radian. In particular C_1 represents the dipole term and this is related to dipole amplitude D as (Gibelyou & Huterer 2012),

$$C_1 = \frac{4\pi}{9} D^2. \tag{10}$$

4.1. Analysis Method and Bias simulation

We do not have data for $\delta \leq 40^\circ$ and we impose a cut $|b| > 15^\circ$ in order to eliminate the region around the Galactic plane. The dipole power of the real data is obtained by filling these empty pixels isotropically by randomly generated data and computing the corresponding full sky power. We generate a total of 1000 realizations of real map by filling the empty pixels with different random samples. The dipole power, C_1', and direction parameters (θ', ϕ'), along with their error, are computed from the corresponding distribution. The dipole extracted in this manner would differ from that extracted from the full sky map, i.e. if real data in all the pixels were available, by some constant k (Singal 2011), which would depend on the mask used for the data. Similarly the extracted values of the direction would also contain a bias. Let (θ, ϕ) represent the true direction of the dipole and (θ', ϕ') the dipole extracted after filling the masked region by isotropic random samples. The bias in the angles is given by, $\Delta\theta = \theta' - \theta$ and $\Delta\phi = \phi' - \phi$. We calculate the constant k and the bias in direction by simulations. The bias corrected value of the dipole power, C_1, is given by, $C_1 = C_1^{'}/k^2$. Similarly the angle parameters of the dipole direction are given by, $\theta = \theta' - \Delta\theta$ and $\phi = \phi' - \Delta\phi$.

The bias is computed by simulating a random sample of radio sources which has the same distribution as the real sources. The simulated sample has a dipole of same strength as seen in real NVSS data in roughly the same direction as observed. These samples are generated by randomly allocating sources to different positions in the sky. Alternatively one may generate these samples by

randomly shuffling data among different pixels. We have verified that these two procedures produce similar results. The pixels in the masked regions $\delta \leq -40^\circ$ and Galactic plane within the latitude $|b| < 15^\circ$, are filled isotropically, as in the case of real data. This provides a particular random sample with same characteristics as the real data. The results obtained from 1000 realizations for source intensity and number dipole are shown in Fig. 2, 3 respectively. These figures show the distribution of k, $\Delta\theta$ and $\Delta\phi$. The resulting mean values of k, $\Delta\theta$ and $\Delta\phi$ over 1000 random samples represent their bias values. The extracted values of k, $\Delta\theta$ and $\Delta\phi$, both for source count and flux density, are shown in Table 1 for different cuts on $S > S_{low}$. The value of k is not too different from unity and the extracted bias in angles is close to zero. Hence the required bias correction is relatively small. We point out that only the mean values of the estimated bias given in Table 1 are relevant, since the parameters in the real sample are also estimated by taking a mean over 1000 realizations of randomly filled masked regions.

$S_{\rm low}$	Sources	Source Counts			Flux density S_I		
		k	$\Delta\theta$	$\Delta\phi$	k	$\Delta\theta$	$\Delta\phi$
10	428210	0.85 ± 0.14	-8.9 ± 16.0	8.8 ± 14.6	0.95 ± 0.24	-9.5 ± 24.7	8.3 ± 24.3
20	240772	0.88 ± 0.18	-9.2 ± 19.5	9.1 ± 19.0	0.97 ± 0.26	-9.2 ± 24.3	9.3 ± 26.6
30	165206	0.91 ± 0.21	-9.4 ± 22.4	9.7 ± 22.0	1.01 ± 0.28	-8.8 ± 27.5	9.6 ± 29.4
40	124173	0.95 ± 0.24	-9.9 ± 24.2	10.3 ± 24.9	1.06 ± 0.32	-9.3 ± 28.6	9.3 ± 31.6
50	98295	0.99 ± 0.27	-9.9 ± 27.0	10.7 ± 27.6	1.09 ± 0.34	-10.6 ± 30.4	12.6 ± 32.9

Table 1: The values of k, $\Delta\theta$ and $\Delta\phi$ extracted from simulations corresponding to source counts and flux density, S_I. These values correspond to the bias generated in the dipole amplitude and direction due to the filling of masked sky with randomly generated data.

The significance of dipole is calculated as follows. We generate 1000 isotropic random realizations by shuffling real data among difference pixels and calculate the corresponding dipole power, $\tilde{C}_1$. The significance, i.e. σ value, represents the deviation of the data C_1' from the power $\tilde{C}_1$ corresponding to random data. Here we use the dipole power, C_1', without applying bias correction since it provides a conservative estimate of significance.

5. Results

In Fig. 4, we show the distribution of C_1' for real data as well as randomly generated simulated data with the cut $S > 20$ mJy for the case of number counts. The corresponding graphs for flux density, S_I, are shown in Fig. 5. Here the flux density is summed over all the sources in a particular pixel. The extracted values of C_1' for various cuts (S>10, 20, 30, 40, 50 mJy) for the case of number count and flux density, S_I, are given in Table 2, 3. In all cases we impose an upper limit $S < 1000$ mJy on the flux density of a source. The cut $S > 10$ mJy is not supposed to be reliable due to the bias in the number counts (Blake & Wall 2002). We show it here mainly for comparison to see how the results change as we push the limit on S to lower values. Hence the results for this

cut should be interpreted cautiously. The significance (σ) of the detected dipole anisotropy as well as the direction parameters (θ', ϕ') are also shown. The primes on these parameters indicate that these have not been corrected for bias. We find that the dipole anisotropy is very significant in the number counts with the maximum value $\sigma \approx 5.4$ for the cut $S_{low} = 20$ mJy. For the flux density (S_I) the maximum value of sigma is found to be about 3.

$S_{\rm low}$	$C_1' \left(\times 10^4\right)$	$\tilde{C}_1 \left(\times 10^4\right)$	σ	$\theta'(^\circ)$	$\phi'(^\circ)$
10	1.278 ± 0.353	0.266 ± 0.213	4.74	73.6 ± 12.0	146.1 ± 8.8
20	2.527 ± 0.672	0.456 ± 0.384	5.39	102.6 ± 10.5	155.8 ± 8.5
30	3.095 ± 0.863	0.620 ± 0.495	5.00	101.4 ± 11.4	159.1 ± 8.5
40	3.103 ± 1.148	0.825 ± 0.626	3.64	117.7 ± 12.0	153.0 ± 10.8
50	4.032 ± 1.414	1.026 ± 0.801	3.75	118.7 ± 10.8	166.4 ± 8.5

Table 2: The extracted value of the dipole power C_1' and the corresponding value for simulated isotropic data $\tilde{C}_1$ using number counts for different cuts on flux density of a source ($S > S_{low}$). The significance of the dipole anisotropy, σ, as well as the extracted polar angles of the dipole axis, θ' and ϕ' are also shown.

$S_{\rm low}$	$C_1' \left(\times 10^4\right)$	$\tilde{C}_1 \left(\times 10^4\right)$	σ	$\theta'(^\circ)$	$\phi'(^\circ)$
10	3.055 ± 0.942	0.728 ± 0.609	3.82	93.6 ± 14.2	161.8 ± 9.6
20	3.842 ± 1.224	0.979 ± 0.829	3.45	98.1 ± 14.1	162.7 ± 9.5
30	4.255 ± 1.396	1.172 ± 0.910	3.39	97.4 ± 14.8	163.1 ± 9.5
40	4.319 ± 1.579	1.341 ± 1.102	2.70	100.7 ± 15.9	161.9 ± 10.3
50	4.855 ± 1.753	1.459 ± 1.156	2.94	100.5 ± 15.8	164.9 ± 9.6

Table 3: The extracted value of the dipole power, C_1', and the corresponding value, $\tilde{C}_1$, for random isotropic data using flux density, S_I, for different cuts ($S > S_{low}$). The significance of the dipole anisotropy, σ, as well as the extracted polar angles of the dipole axis, θ' and ϕ' are also shown.

After correcting for bias, the extracted dipole amplitudes, $|\vec{D}_N(obs)|$ and $|\vec{D}_S(obs)|$, corresponding to number counts and flux density respectively, are shown in Tables 4, 5. The extracted speed of the solar system and angles (θ, ϕ), after correcting for bias, are also shown. The value of x in Eqs. 2 and 3 is obtained by directly fitting the data. We find $x = 0.759, 0.885, 0.959, 1.018, 1.062$ for the cuts $S > 10, 20, 30, 40$ and 50 mJy respectively. We find that, for the case of number counts, the results show some variation with the cut on flux density. However the change is not very large and the results agree within errors, as long as we ignore the cut $S > 10$ mJy. For such small values of flux density, the data is known to have uneven distribution of source counts due to non-uniform sampling (Blake & Wall 2002). The corresponding parameters extracting using flux density are found to be comparatively insensitive to the cut imposed. The angle parameters show almost no change, whereas the extracted speed varies between 896.8 ± 163.86 to 967.3 ± 154.10, including the

cut $S > 10$ mJy. The extracted speed is found to be about 2.5 times the expectation from CMBR observations. The significance of the difference is about 3.5σ. For number counts the significance is larger, about $4 - 5\ \sigma$, depending on the cut. Hence the data is not consistent with the CMBR dipole. It clearly indicates the presence of an intrinsic dipole anisotropy which cannot be explained in terms of local motion. The result corresponding to flux density, S_I, is particularly interesting due to its relative insensitivity to the cut on S.

$S_{\rm low}$	$\vert\vec{D}_N\vert$	$\vec{v}$		
		$\vert\vec{v}\vert$	$\theta\ (^o)$	$\phi\ (^o)$
10	0.0113 ± 0.0016	1018 ± 141	82 ± 12	137 ± 9
20	0.0153 ± 0.0020	1291 ± 172	112 ± 10	147 ± 8
30	0.0163 ± 0.0023	1329 ± 185	111 ± 11	149 ± 9
40	0.0157 ± 0.0029	1244 ± 230	128 ± 12	143 ± 11
50	0.0172 ± 0.0030	1340 ± 235	129 ± 11	156 ± 9

Table 4: The extracted dipole amplitude $\vert\vec{D}_N(obs)\vert$ for different cuts, after correcting for bias. The corresponding parameters of the velocity vector, $\vec{v}$, of the solar system are also shown.

$S_{\rm low}$	$\vert\vec{D}_S\vert$	$\vec{v}$		
		$\vert\vec{v}\vert$	$\theta\ (^o)$	$\phi\ (^o)$
10	0.0155 ± 0.0024	917 ± 141	103 ± 14	153 ± 10
20	0.0171 ± 0.0027	967 ± 154	107 ± 14	153 ± 9
30	0.0172 ± 0.0028	951 ± 156	106 ± 15	153 ± 10
40	0.0165 ± 0.0030	897 ± 164	110 ± 16	153 ± 10
50	0.0171 ± 0.0031	917 ± 166	111 ± 16	152 ± 10

Table 5: The dipole amplitude, $\vert\vec{D}_S(obs)\vert$, extracted from flux density, S_I, for different cuts, after correcting for bias. The corresponding parameters of the velocity vector, $\vec{v}$, of the solar system are also shown.

The results for the extracted intrinsic dipole, $\vec{D}_0$, and the corresponding kinematic dipole, based on the model prescribed by Eqs. 4 and 5, are given in Table 6. The results have a relatively large error and also show significant dependence on the cut. The extracted speed still turns out to be large in comparison to the expectation based on CMBR dipole. Due to large error, however, the deviation is significant only at a little more than 1 σ. The extracted intrinsic dipole is significant at 3 σ. The dependence on cut and the large error most likely arise due to large fluctuations in the data. We expect that with larger data this method may be utilized more effectively.

6. Discussion and Conclusion

We qualitatively confirm the results obtained in (Singal 2011). We find that the dipole anisotropy, both in number count and flux density, cannot be consistently interpreted in terms of the local motion of the solar system, as derived by the CMBR measurements. The difference is significant at $4-5\ \sigma$ for number counts, depending upon the cut and at $2.5\ \sigma$ for sky brightness. The results for the case of sky brightness are relatively insensitive to the cut imposed. The significance of detection of the dipole anisotropy is found to be about $3\ \sigma$ from flux density and $3.6-5.4\ \sigma$ for number counts. This parameter was not quoted in earlier papers. Our extracted speed is considerably smaller in comparison to Singal (2011) for the case of flux density. For number counts it is also smaller, but the difference is not very significant. The difference for the case of flux density may be partially attributed to the additional factor of $(1+\alpha)$ present in the formula, Eq. 3, which relates the dipole amplitude to speed. This factor has been missed in earlier papers. In part the difference might arise due to the procedure used in extracting the dipole. We make a spherical harmonic decomposition of the data, which isolates the dipole contribution. In contrast the procedure used in (Singal 2011) would also get contributions from higher multipoles, which may be small but not completely negligible.

The results we obtain with flux density are remarkably stable. The dispersion seen is much smaller than that seen in (Singal 2011). Even for the cut $S > 10$ mJy, the results obtained are consistent with those obtained with other cuts. Excluding $S > 10$ mJy, the results obtained with number counts are also relatively insensitive to the cut. The deviation seen for $S > 10$ mJy is understandable due to bias present at low flux densities (Blake & Wall 2002). This insensitivity gives us more confidence that the anisotropy we observe may have a physical origin. It is reasonable that the results for flux density show less scatter in comparison to source counts since the fluctuations induced due to sources with low flux density get reduced. Finally, assuming the presence of an intrinsic dipole contribution in the source counts, we separate it out from the kinematic dipole. The resulting speed of the solar system, however, is still found to be higher than the CMBR expectation. Our results support the hypothesis that the Universe is intrinsically anisotropic with the anisotropy axis pointing towards Virgo (Jain & Ralston 1998; Ralston & Jain 2004).

$S_{\rm low}$	D_0	$\theta_I(^\circ)$	$\phi_I(^\circ)$	v	$\theta(^\circ)$	$\phi(^\circ)$
10	0.0164 ± 0.0057	47 ± 22	86 ± 45	1318 ± 330	128 ± 21	193 ± 26
20	0.0160 ± 0.0053	115 ± 27	127 ± 27	835 ± 320	84 ± 38	201 ± 47
30	0.0181 ± 0.0056	115 ± 24	136 ± 23	771 ± 328	78 ± 41	205 ± 64
40	0.0216 ± 0.0068	145 ± 20	104 ± 48	1122 ± 345	57 ± 26	197 ± 34
50	0.0238 ± 0.0071	152 ± 15	173 ± 40	1034 ± 402	42 ± 29	157 ± 58

Table 6: The extracted intrinsic dipole amplitude D_0, the corresponding direction parameters (θ_I, ϕ_I) and the kinematic dipole parameters (v, θ, ϕ) for various cuts on the flux density.

Acknowledgements

We have used CERN ROOT 5.27 for generating our plots. Some of the results in this paper have been derived using the HEALPix (K.M. Górski et al., 2005, ApJ, 622, p759) package. Prabhakar Tiwari and Rahul Kothari sincerely acknowledge CSIR, New Delhi for the award of fellowship during the work.

REFERENCES

Blake, C., & Wall, J. 2002, Nature, 416, 150

Condon, J. J., Cotton, W. D., Greisen, E. W., et al. 1998, The Astronomical Journal, 115, 1693

Corwin, Jr., H., Buta, R., & de Vaucouleurs, G. 1994, The Astronomical Journal, 108, 2128

de Oliveira-Costa, A., Tegmark, M., Zaldarriaga, M., & Hamilton, A. 2004, PhRvD, 69, 063516

Ellis, G. F. R., & Baldwin, J. E. 1984, Mon.Not.Roy.Astron.Soc., 206, 377

Gibelyou, C., & Huterer, D. 2012, Mon.Not.Roy.Astron.Soc., 427, 1994

Hutsemékers, D. 1998, A&A, 332, 410

Hutsemékers, D., & Lamy, H. 2001, A&A, 367, 381

Jain, P., Narain, G., & Sarala, S. 2004, MNRAS, 347, 394

Jain, P., & Ralston, J. P. 1998, MPLA, 14, 417

Kashlinsky, A., Atrio-Barandela, F., Kocevski, D., & Ebeling, H. 2009a, ApJ, 686, L49

—. 2009b, ApJ, 691, 1479

Ralston, J. P., & Jain, P. 2004, IJMPD, 13, 1857

Saunders, W., Sutherland, W., Maddox, S., et al. 2000, Mon.Not.Roy.Astron.Soc., 317, 55

Schwarz, D. J., Starkman, G. D., Huterer, D., & Copi, C. J. 2004, Phys. Rev. Lett., 93, 221301

Singal, A. K. 2011, ApJL, 742, L23

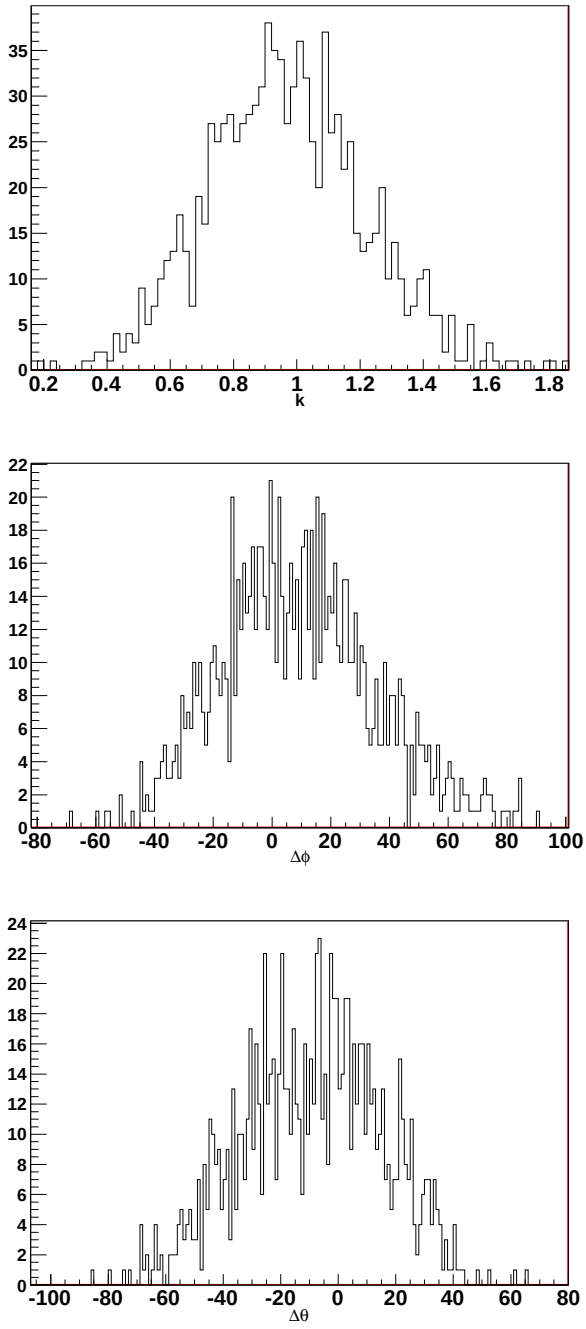

Fig. 2.— Estimating the bias from simulations: The distribution of $k = \sqrt{C_1'/C_1}, \Delta\theta = \theta' - \theta$ and $\Delta\phi = \phi' - \phi$ for flux density with the cut, $S > 20$ mJy. Here unprimed quantities denote the values from the full sky simulated data and primed quantities denote the values extracted by identifying masked regions in the simulated data and replacing them by the filling procedure.

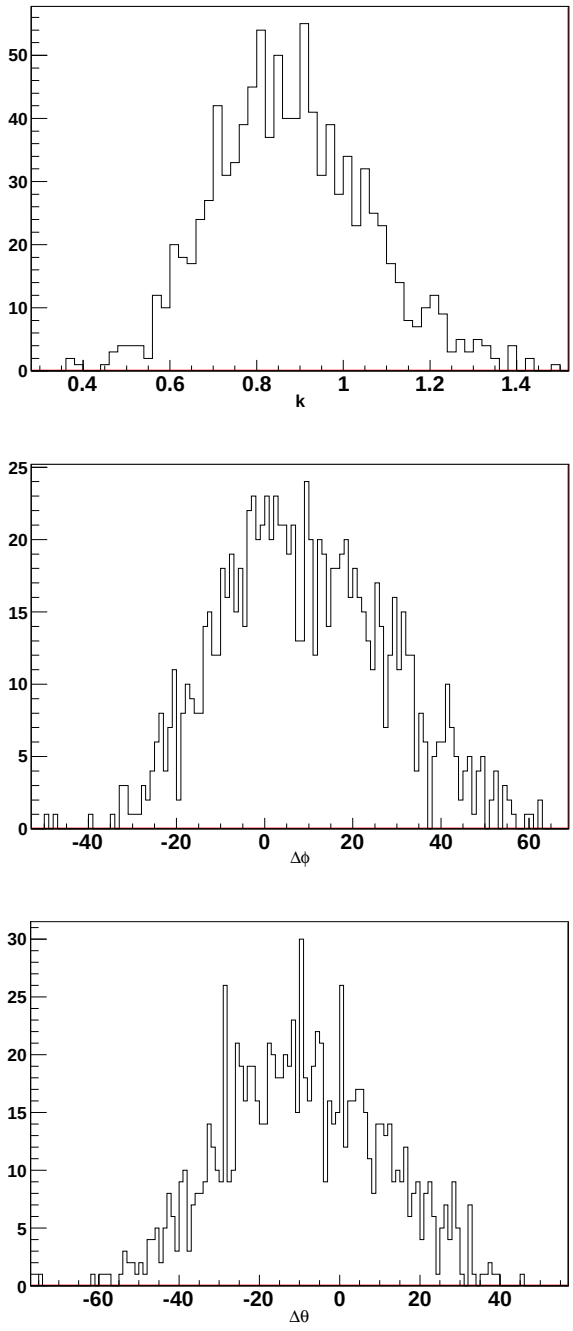

Fig. 3.— The distribution of bias parameters $k = \sqrt{C_1'/C_1}, \Delta\theta = \theta' - \theta$ and $\Delta\phi = \phi' - \phi$ for source counts ($S > 20$ mJy), extracted by simulations.

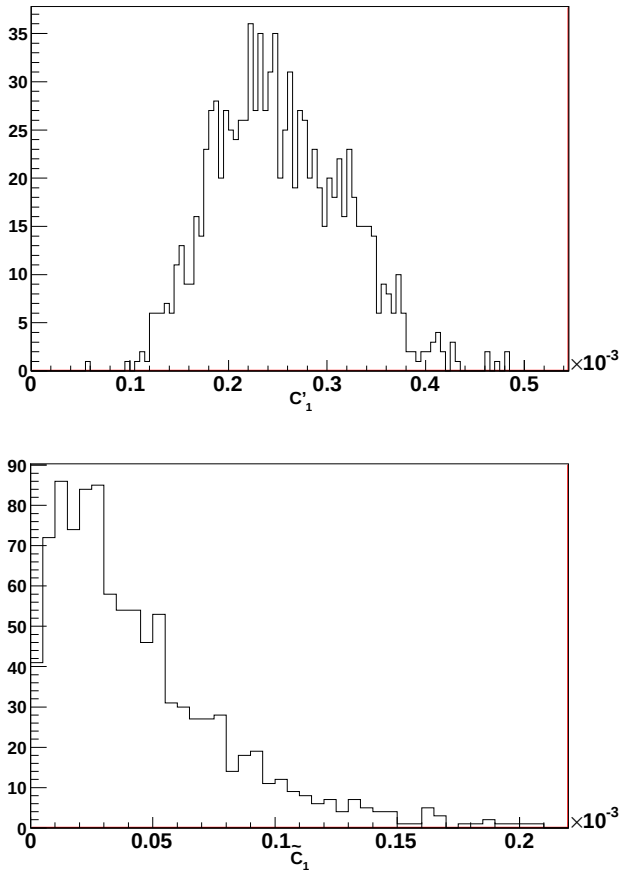

Fig. 4.— The distribution of dipole power for number count of sources for the case of real data (upper graph) and random simulated data (lower graph) for sources with flux density greater than 20 mJy. The distribution of real data is obtained by randomly filling in the masked regions, as explained in text.

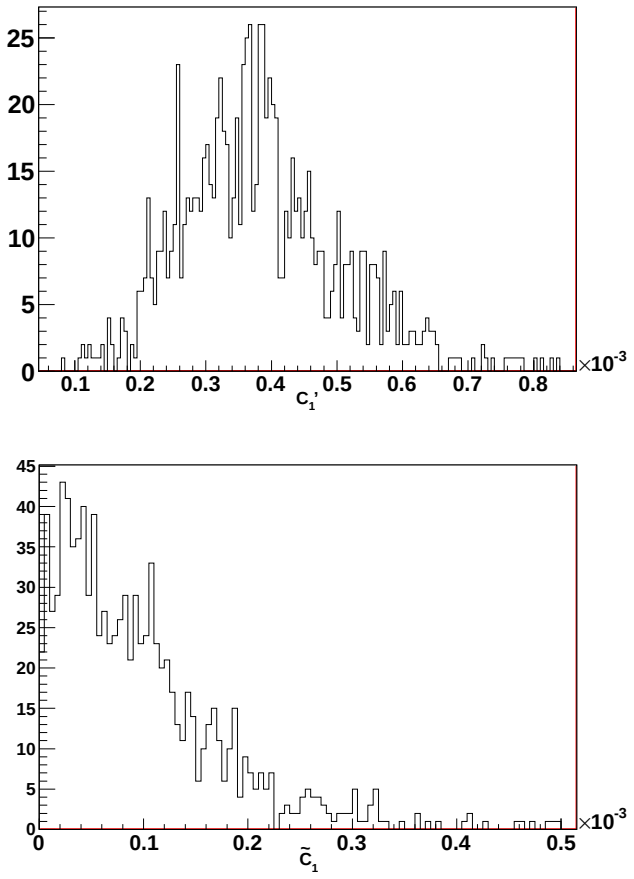

Fig. 5.— The distribution of dipole power for flux density of sources for the case of real data (upper graph) and random simulated data (lower graph) for sources with flux density greater than 20 mJy. The distribution of real data is obtained by randomly filling in the masked regions, as explained in text.